

Measurement of Higgs boson production at high transverse momentum in the $VH, H \rightarrow b\bar{b}$ channel with the ATLAS detector

Brian Moser*, on behalf of the ATLAS Collaboration

Nikhef,

Science Park 105, 1098 XG Amsterdam, The Netherlands

E-mail: brian.moser@cern.ch

With the rapidly increasing proton-proton collision data set provided by the LHC, the ATLAS experiment gains access to Higgs bosons produced with ever higher transverse momenta p_T^H . Measurements in this phase space are well motivated by a vast variety of BSM models which predict effects that scale with the square of the involved energy scale. The associated production of a Higgs boson H with a heavy vector boson V contributes significantly to the total production cross-section at high p_T^H . Combining this production mode with the most prominent decay into a pair of b-quarks promises a large enough signal yield in this rare topology. A novel measurement of the production cross-section times the decay branching-fraction for this process is presented, based on data collected between 2015 and 2018 at a center-of-mass energy of 13 TeV. Results are provided in two fiducial regions of the transverse momentum of the vector boson: $250 \text{ GeV} < p_T^V < 400 \text{ GeV}$ and $p_T^V \geq 400 \text{ GeV}$. These cross-sections are furthermore interpreted as limits on the Wilson coefficients of a Standard Model Effective Field Theory.

*40th International Conference on High Energy physics - ICHEP2020
July 28 - August 6, 2020
Prague, Czech Republic (virtual meeting)*

*Speaker



The precise determination of the Higgs boson's properties is one of the main pillars in the physics program of the ATLAS experiment [1]. Using pp -collision data collected during the second operational run of the LHC from 2015 to 2018, the rates of the main production modes and decay channels have been determined with great precision. The large data set, corresponding to an integrated luminosity of 139 fb^{-1} , furthermore allows to study differential quantities, such as the transverse momentum distribution of the Higgs boson $d\sigma/dp_{\text{T}}^H$. Measurements at high p_{T}^H are of interest because of their enhanced sensitivity to physics beyond the Standard Model (SM).

At large transverse momentum, the associated production of a Higgs boson H with a heavy vector boson $V(=W, Z)$ contributes significantly to the total production cross-section [2]. Here, a novel measurement of this production mode at high energies by targeting the most prominent Higgs boson decay channel, i.e. $VH, H \rightarrow b\bar{b}$, is presented [3]. An earlier measurement of this channel [4] aimed at reconstructing both of the b -jets from the Higgs boson decay separately, using two anti- k_t jets with a radius parameter $R = 0.4$. For $p_{\text{T}}^H > 300 \text{ GeV}$, however, a significant fraction of b -jet pairs are geometrically too close to be reconstructed separately. To explore Higgs production in this 'boosted' regime, a different approach is taken here, using a single anti- k_t calorimeter jet with $R = 1.0$ to reconstruct Higgs boson candidates. Flavor tagging is performed on track-jets with a p_{T} -dependent radius parameter that are associated to this ($R = 1.0$) jet.

To maximize trigger efficiency and signal purity, only leptonic decays of the vector boson are considered. The targeted final state signatures are $ZH \rightarrow \nu\nu b\bar{b}$, $WH \rightarrow \ell\nu b\bar{b}$ and $ZH \rightarrow \ell\ell b\bar{b}$ ($\ell = \text{muon or electron}$). Events are categorized according to their charged lepton multiplicity into a 0-, a 1- and a 2-lepton channel. Further event selection criteria are applied to reduce the background contamination from W - and Z -jets, $t\bar{t}$, single-top, diboson and QCD multijet production [3]. Signal candidate events are categorized in two kinematic regions, $250 \text{ GeV} < p_{\text{T}}^V < 400 \text{ GeV}$ and $p_{\text{T}}^V \geq 400 \text{ GeV}$, where the transverse momentum p_{T}^V of the reconstructed vector boson was chosen as kinematic variable over p_{T}^H because of its higher experimental resolution. Events are further categorized according to the number of additional $R = 0.4$ calorimeter jets and the number of additional b -tagged track-jets in the event to enhance the sensitivity to the VH signal. In total, ten signal regions and 4 $t\bar{t}$ control regions are considered.

A binned profile likelihood fit to the invariant large- R jet mass m_J is used to simultaneously extract the signal strength $\mu_{VH}^{b\bar{b}}$ with that of diboson production ($\mu_{VZ}^{b\bar{b}}$), where all signal strengths are defined as the yields relative to the SM expectation. The measured values

$$\mu_{VZ}^{b\bar{b}} = 0.91 \pm 0.15(\text{stat.})_{-0.17}^{+0.25}(\text{syst.}) \quad \text{and} \quad \mu_{VH}^{b\bar{b}} = 0.72_{-0.28}^{+0.29}(\text{stat.})_{-0.22}^{+0.26}(\text{syst.})$$

agree with the SM within their uncertainties. Figure 1 (left) shows the distribution of the invariant mass m_J summed over all signal regions, weighted by their respective fitted signal-to-background ratio. Additionally, cross-section measurements are performed within the framework of simplified template cross-sections [5] in two fiducial regions of simulated transverse vector boson momentum: $250 \text{ GeV} < p_{\text{T}}^V < 400 \text{ GeV}$ and $p_{\text{T}}^V \geq 400 \text{ GeV}$, where the latter is measured exclusively for the first time. The results are shown in Figure 1 (right) and are limited by statistical uncertainties.

The cross-section measurements are further interpreted in terms of constraints of Wilson co-

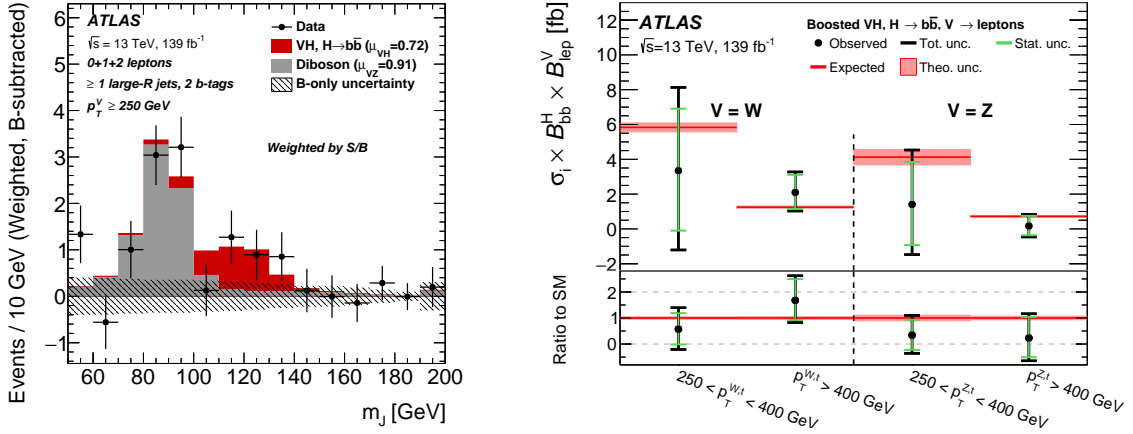


Figure 1: Left: The m_J distribution in data after subtracting all simulated backgrounds except for the WZ and ZZ processes. All signal regions are summed and weighted by their respective fitted signal-to-background ratio. Right: Measured and SM predicted cross-sections times branching fractions in kinematic regions defined at the particle level (STXS-1.2). All results taken from Ref. [3].

efficients corresponding to dimension-6 operators of a SM Effective Field Theory. Following the methodology of Ref. [6], limits are set on individual coefficients of the Warsaw basis, including only terms that are linear in the SMEFT operators, or alternatively, also including quadratic terms of these operators. Figure 2 demonstrates the impact of the measurement split at $p_T^V = 400$ GeV on the limits for the $c_{Hq}^{(3)}$ coefficient, which parametrizes a p_T^V -dependent effect. The additional granularity improves the constraints by nearly a factor two. Furthermore, for the linear parametrization, combinations of Wilson coefficients that can be fit simultaneously are identified via a Principal Component Analysis and subsequently constrained [3]. The most sensitive combinations consist of coefficients associated to operators that induce effects that increase with p_T^V . The leading one is nearly identical to $c_{Hq}^{(3)}$ and can be constrained up to ~ 0.06 TeV^{-2} at 95% CL.

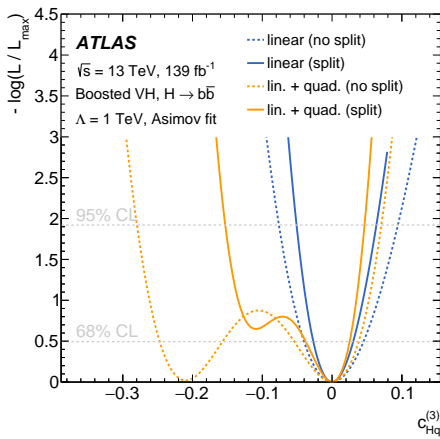


Figure 2: Expected negative log-likelihood profile as a function of $c_{Hq}^{(3)}$ using the two p_T^V bins of the analysis (solid) and using a single bin of $p_T^V > 250$ GeV (dashed). All other Wilson coefficients are fixed to zero. Taken from Ref. [3].

References

- [1] ATLAS Collaboration, *JINST* **3** (2008), S08003 doi:10.1088/1748-0221/3/08/S08003
- [2] K. Becker *et al.*, arXiv:2005.07762
- [3] ATLAS Collaboration, arXiv:2008.02508
- [4] ATLAS Collaboration, arXiv:2007.02873
- [5] LHC Higgs Cross Section Working Group, doi:10.23731/CYRM-2017-002 arXiv:1610.07922
- [6] ATLAS Collaboration, ATL-PHYS-PUB-2019-042, <https://cds.cern.ch/record/2694284>